A seismic array on Mt. Vesuvius

<u>Partecipant institutions</u>

Osservatorio Vesuviano

Edoardo Del Pezzo, Francesca Bianco, Mario Castellano, Simona Petrosino, Folco Pingue, Marco Capello, Teodoro Esposito, Vincenzo Augusti.

Dipartimento di Fisica - Università di Salerno

Gilberto Saccorotti, Mario La Rocca, Rosalba Maresca, Danilo Galluzzo, Alessandra Cirillo, Bernardo Grozea.

Instituto Andaluz de Geofisica - Universidad de Granada

Jesus Ibanez, Enrique Carmona, Gerardo Alguacil.

Osservatorio Vesuviano

Open file report

1999 n° 1

Abstract

In November 1997 a seismic antenna (array) of short period seismometers was installed on the south-western flank of Mt. Vesuvius; aim of the experiment was to test the use of non-conventional devices for the seismic monitoring of this volcano. In 7 months local seismicity, regional earthquakes and samples of seismic noise were recorded by the array and organised in a data base.

Local earthquakes and seismic noise have been analysed with array techniques to investigate the spectral, kinematic and polarization properties of the wavefield. Preliminary results show that the backazimuth of local earthquakes is oriented in the direction of the crater area. For some events, the source location has been constrained using a simplified back propagation in a 2-D velocity structure.

The noise wavefield is characterized by the predominance of a sustained low frequency component (< 1Hz) whose source is located S-SE of the array. This low frequency signal has been interpreted as associated to the sea-loading in the gulf of Naples.

Introduction

Seismic arrays have been widely used (Goldstein & Chouet, 1994; Ferrazzini et. al., 1991; Dietel et al.,1994; Del Pezzo et. al, 1997) to study the wavefield associated to volcanic activity and many analyses have shown how array techniques are useful for the discrimination of the different seismic phases. In volcanic areas, the seismograms are very complex due to the topography and the heterogeneity of the medium in which seismic waves propagate: for this reason it is difficult to discriminate seismic phases in the wavefield associated to earthquakes. As a consequence of this problem, the S-wave arrival time picking is affected by a large error which causes an inaccurate and approximate location of the earthquakes. Moreover the misidentification of the seismic phases may lead to an inexact interpretation both of the source excitation mechanisms and of the later arrivals associated to the propagation in heterogeneous media.

In this framework, the application of array techniques to the seismicity recorded by the digital antenna can improve the results of the analyses (such as location of the source and polarization analysis) which are routinely performed on the data recorded by the Osservatorio Vesuviano seismic network.

Array techniques are also applied to some samples of seismic noise recorded during the experiment to investigate the spectral characteristics and the directional properties of the noise wavefield. This kind of analysis aims at the discrimination of possible insurgent volcanic tremor which can be a probable precursor of volcanic eruptions.

Instruments and data recording

The array was located in the National Park of Mt. Vesuvius in the Baracche Forestali area, at a distance of about 1.5 Km from the crater (fig. 1). It was formed by 18 vertical geophones Mark L15B (600 ohm coil resistance) and 2 three component geophones Mark L15B (380 ohm coil resistance). The natural frequency (4.5 Hz) of the seismometers was electronically extended to 1 Hz. Sensors were buried in approximately 30 cm deep holes. The 3-D sensors were deployed with the horizontal components oriented in the N-S and E-W directions. Sensor coordinates were measured using differential GPS positioning, with a precision of about 30 cm in absolute sensor location(fig.1 , tab.1).

In the last week of operation four sensors were moved to the centre of the array to obtain a new configuration (fig.2, tab 2) more suitable for the study of the seismic noise.

The altitude difference among the sensors was less than 80 meters and the maximum aperture was about 500 meters. Although the array was deployed on the volcano flank, the average slope was about 10 degrees; this particular deployment allows the planar geometry approximation.

Station	Lat.	Long.	Lat. (m)	Long. (m)	Elev. (m)
1B	40 48 41.976 N	14 24 41.909 E	307.6	325.9	658
1C	40 48 37.892 N	14 24 36.662 E	81.7	203	645
1D	40 48 39.692 N	14 24 38.969 E	237.2	257.1	652
2D	40 48 37.734 N	14 24 33.438 E	176.8	127.4	633
3D	40 48 39.462 N	14 24 35.656 E	230.1	179.4	645
4B	40 48 40.678 N	14 24 40.096 E	267.6	283.4	654
4C	40 48 35.302 N	14 24 31.739 E	101.8	87.7	624
4D	40 48 40.306 N	14 24 28.350 E	256.1	8.2	630
5B	40 48 44.945 N	14 24 46.544 E	399.1	434.5	686
5C	40 48 34.481 N	14 24 34.927 E	76.5	162.3	622
5D	40 48 43.328 N	14 24 35.764 E	349.3	181.9	651
6B	40 48 40.713 N	14 24 46.076 E	268.6	423.6	672
6C	40 48 37.129 N	14 24 38.144 E	158.1	237.7	637
6D	40 48 42.421 N	14 24 38.282 E	321.3	241	661
7B	40 48 37.448 N	14 24 41.261 E	168	310.8	650
7C	40 48 32.725 N	14 24 36.572 E	22.4	200.9	613
7D	40 48 46.447 N	14 24 38.667 E	445.4	250	662
8B	40 48 36.385 N	14 24 46.803 E	135.2	440.6	661
8C	40 48 35.098 N	14 24 42.041 E	95.5	329	634
8D	40 48 45.059 N	14 24 40.621 E	402.6	295.8	702

Table Errore. L'argomento parametro è sconosciuto. - Sensor coordinates (configuration A).

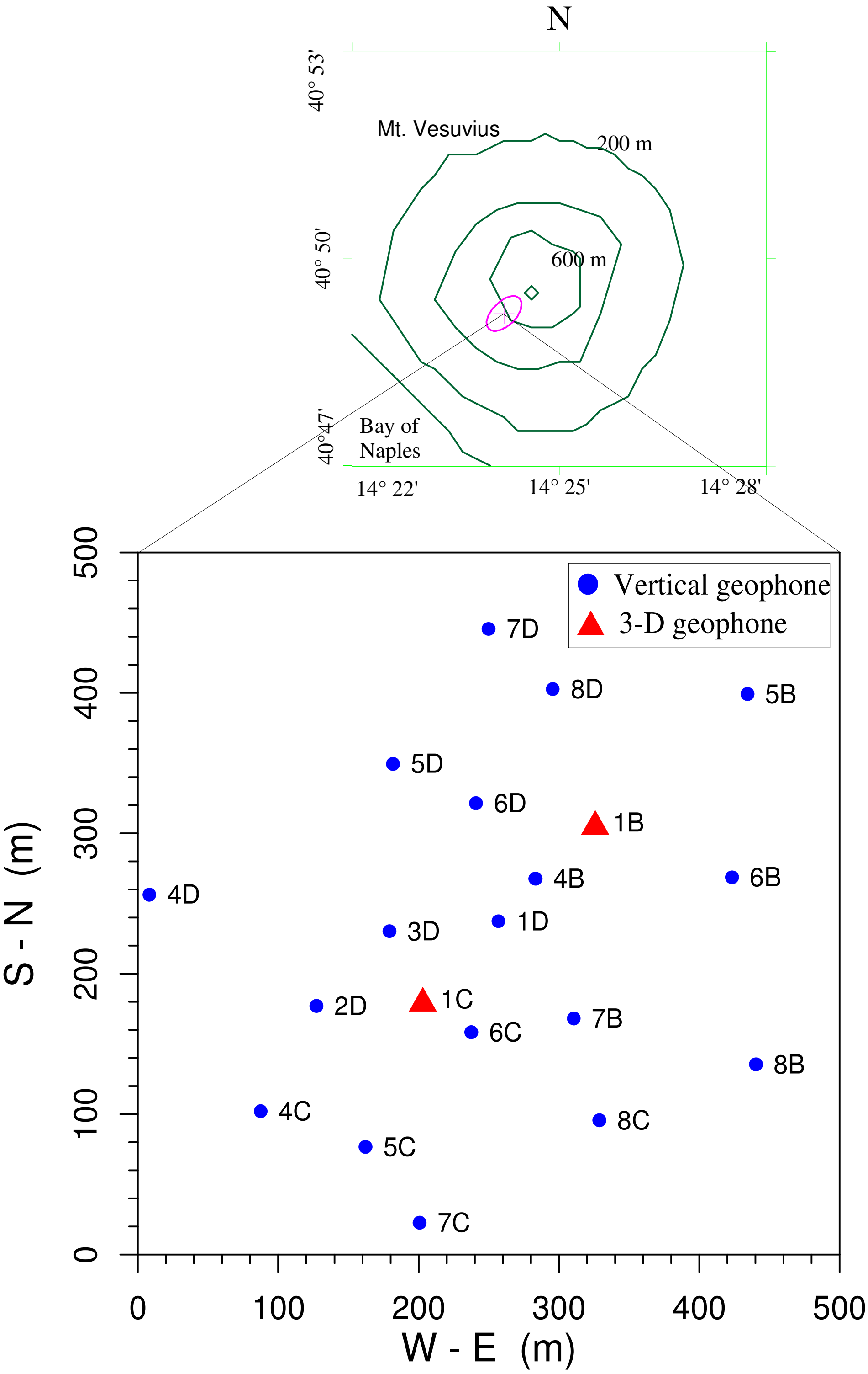

Fig. 1 - Configuration A of the seismic array.

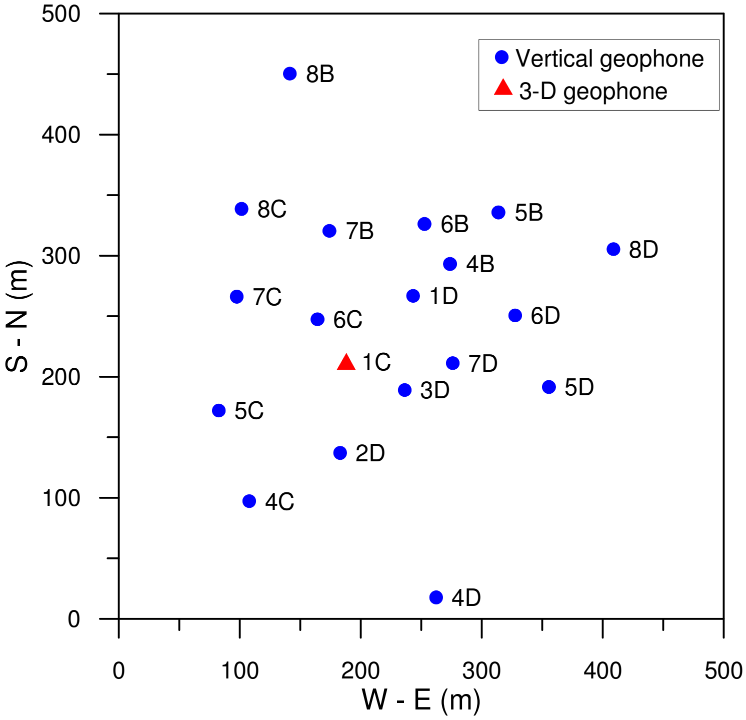

Fig. 2 - Configuration B of the seismic array.

Station	Lat.	Long.	Lat. (m)	Long. (m)	Elev. (m)
1C	40 48 37.892 N	14 24 36.662 E	81.7	203	645
1D	40 48 39.692 N	14 24 38.969 E	237.2	257.1	652
2D	40 48 37.734 N	14 24 33.438 E	176.8	127.4	633
3D	40 48 39.462 N	14 24 35.656 E	230.1	179.4	645
4B	40 48 40.678 N	14 24 40.096 E	267.6	283.4	654
4C	40 48 35.302 N	14 24 31.739 E	101.8	87.7	624
5B	40 48 41.976 N	14 24 41.909 E	307.6	325.9	658
5C	40 48 34.481 N	14 24 34.927 E	76.5	162.3	622
5D	40 48 43.328 N	14 24 35.764 E	349.3	181.9	651
6B	40 48 39.996 N	14 24 41.505 E	268.6	423.6	653
6C	40 48 37.129 N	14 24 38.144 E	158.1	237.7	637
6D	40 48 42.421 N	14 24 38.282 E	321.3	241	661
7B	40 48 37.448 N	14 24 41.261 E	168	310.8	650
7C	40 48 34.968 N	14 24 38.945 E	22.4	200.9	631
7D	40 48 40.748 N	14 24 36.602 E	445.4	250	655
8C	40 48 35.098 N	14 24 42.041 E	95.5	329	634
8D	40 48 45.059 N	14 24 40.621 E	402.6	295.8	702

Table 2 - Sensor coordinates (configuration B). The geophones 6B, 7C and 7D have been moved from the old position, while the 3-D station 1B was substituted by the geophone 5B.

The sensors, cased in an aluminium box together with the amplifier and the circuit for the dynamical extension, were cable-connected to the data loggers. As the acquisition system can record up to 8 channels, the array was divided into 3 subarrays controlled by 3 distinct data loggers. Each data logger was formed by a 16 bits A/D converter, an anti-aliasing filter and a GPS control circuit connected to a GPS antenna for absolute timing. These components were cased in a plastic box and connected via parallel and serial port to a portable PC. The array acquisition system is a non-commercial one designed by R. Ortiz and G. Alguacil; more information about the instruments as well as details about the electronic schemes can be found in Olmedillas and Ortiz (1990).

The block-diagram of the device and the characteristic parameters of the geophones and pre-amplifier are reported in the following figure and table.

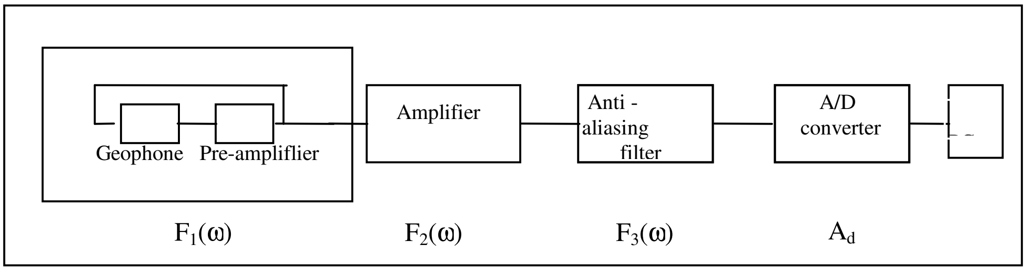

Fig. 3 - Block scheme of the device used for the experiment.

Parameter	L15B 380 Ohm	L15B 600 Ohm
d (damping factor)	3.90	4.06
G (trasduction constant) [Vs/m]	36.06	45.32
M (mass) [Kg]	0.023	0.023
R_c (geophone resistance) [Ohm]	380	600
R (total resistance of the circuit geophone + pre-amplifier) [Ohm]	275.7	422.2
A_v (voltage amplification)	-71.11	-79.02
ω_0 (geophone natural frequency) [Hz]	4.5	4.5

Table 3 - Characterisic parameters of the geophones and pre-amplifier.

The feedback connection between the geophone and the pre-amplifier provides an input signal which is the sum of the ground motion plus an electric signal proportional to the geophone output. This configuration improves the stability of the circuit because the geophone damping factor is incremented by the quantity:

$$\Delta d = \frac{G^2}{2MR\omega_0}$$

and the total damping of the system geophones + pre-amplifier is $D = d + \Delta d$ .The transfer function of the circuit geophone + pre-amplifier is:

$$F_1(\omega) = GA_v \frac{(i\omega)^2}{(i\omega)^2 + 2D\omega_0 i\omega + (\omega_0)^2}$$

where A_v is the voltage amplification.

The pre-amplifier is connected to the amplification circuit which has the following transfer function:

$$F_2(\omega) = \left(1 + \frac{R_4}{R_5}\right) \frac{\frac{i\omega}{\omega_2} + 1}{\frac{i\omega}{\omega_1} + 1}$$

with:

$$\omega_1 = \frac{1}{R_5 C} = 3.61 \text{ rad/s} \qquad \omega_2 = \frac{R_4 + R_5}{R_4 R_5 C} = 227 \text{ rad/s}$$

$R_4 = 9.51$ KΩ $\qquad R_5 = 590$ KΩ $\qquad C = 470$ nF

If $\omega \to \infty$ the function $F_2(\omega) \to 1$, while if $\omega \to 0$ then $F_2(\omega) = 1 + R_4/R_5 \approx 63$. For this reason, the amplification circuit extends the observable frequency range to values lower than 4.5 Hz which is the natural frequency of the geophone.

The anti-aliasing filter is formed by a Butterworth filter and an amplifier and its cut-off frequency is $f_3 = 49.1$ Hz. The transfer function of this circuit (filter + amplifier) is:

$$F_3(\omega) = \frac{a}{\prod_{j=1}^{4} \left[\frac{(i\omega)^2}{\omega_3^2} + 2d_j \frac{i\omega}{\omega_3} + 1 \right]}$$

with $d_1 = 0.98$, $d_2 = 0.82$, $d_3 = 0.59$, $d_4 = 0.20$, $a = 6.687$.

The analogical signal is converted into a digital signal by the A/D converter which gives its contribution to the whole transfer function by a factor:

$$A_d = \frac{2^{16} - 1}{8192} \text{ counts/Volt}$$

Therefore, the total transfer function of the device geophone + acquisition system is:

$$F(\omega) = F_1(\omega) F_2(\omega) F_3(\omega) A_d$$

The modulus of $F(\omega)$ is shown in fig. 4: the particular shape of this function makes the instrument response constant in the 1-50 Hz frequency range.

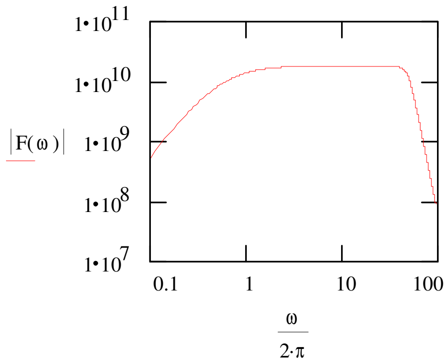

Fig. 4 - The total instrument transfer function.

Seismic signals were recorded using the trigger algorithm (LTA/STA), sampled at 200 samples/s and stored on the PC hard disk. Batteries were changed twice a week and a check of the instruments was made at the same time. Data recorded by the array were transferred once a week from the 3 acquisition PCs on a portable PC and then, after a selection in the seismological laboratory of Università di Salerno, were stored on PC-Zip diskettes. Data are available in PICFASE format (described in Del Pezzo et. al, 1998) and can be read by PICFASE program (Guirao, 1991).

The array operated from November 1997 to June 1998, recording about 450 local earthquakes (among them there were two seismic swarms occurred on January 11th 1998 and March 2nd 1998), some regional earthquakes and some artificial explosions. An example of a local event is shown in fig.6. The number of local earthquakes (fig. 7) recorded by the array in the period November 1997 - June 1998 is higher than that recorded by the Osservatorio Vesuviano seismic network, demonstrating that the digital antenna improves the signal to noise ratio and decreases the detection threshold for local microearthquakes. Samples of seismic noise (fig. 5) were recorded using 215, 120-s-long programmed windows. Of these, 143 were recorded with the geophones deployed in configuration A (fig. 1) and 72 in configuration B (fig.2). A complete list of local and regional earthquakes and seismic noise samples recorded by the array is reported in appendix A.

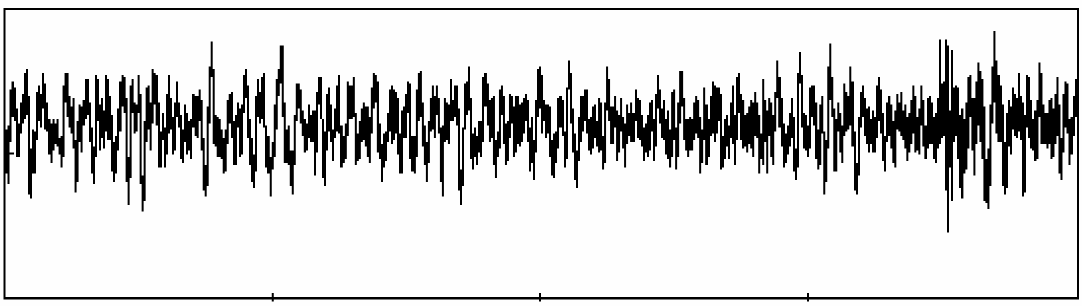

Fig. 5 - 120 s time window of seismic noise recorded by the array.

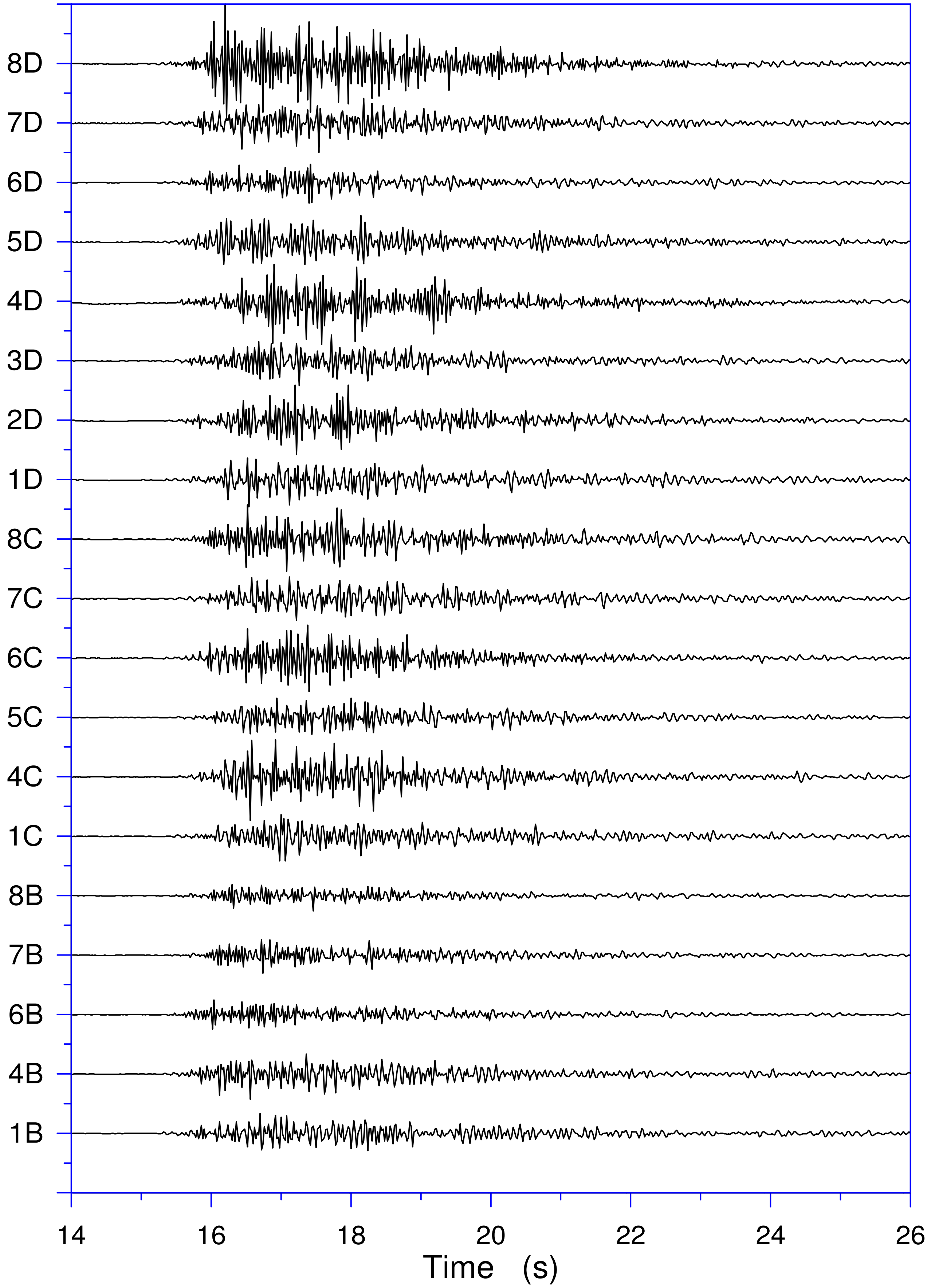

Fig. 6 - Local earthquake 0110355 recorded by the array.

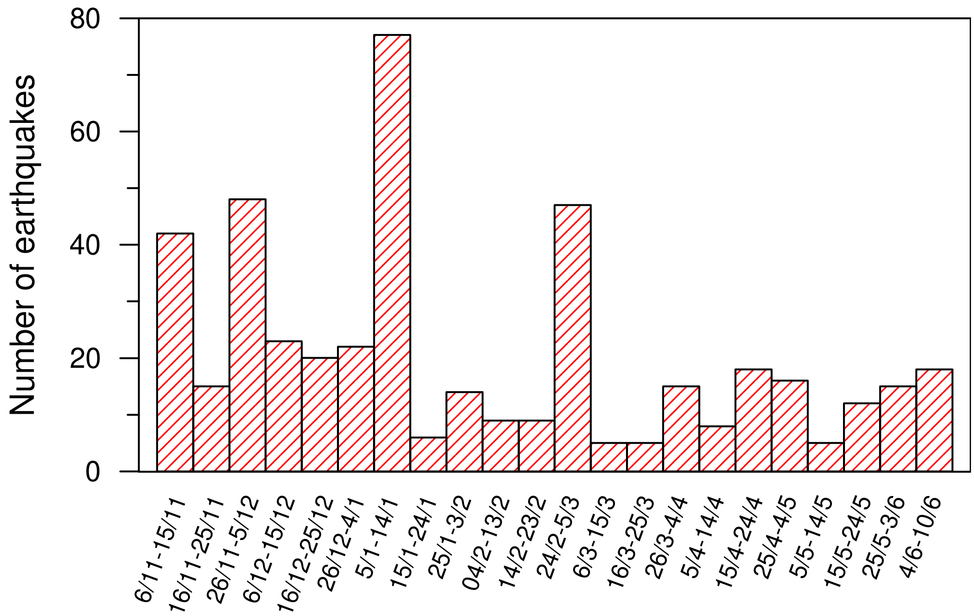

Fig 7 - Distribution of the local earthquakes recorded by the array in the period November 1997 - June 1998.

Data analysis and preliminary results

Local earthquake analysis

The wavefield associated to local earthquakes has been analysed with the zero-lag cross-correlation (ZLCC) technique (Frankel et al., 1991; Del Pezzo et. al, 1997) to estimate horizontal slowness (the inverse of apparent velocity) and backazimuth. An example is shown in fig. 8 where we report the slowness spectrum of the P-wave onset for 8 local events belonging to the seismic swarms mentioned above. In those spectra, the array-averaged zero-lag cross-correlation coefficient is contoured as a function of the two components of the horizontal slowness. The vector which locate the main peak with respect to the spectrum origin gives the apparent velocity and backazimuth of the signal according to the relations:

$$v_{app} = \frac{1}{\sqrt{p_x^2 + p_y^2}} \qquad \varphi = \frac{\pi}{2} - \tan^{-1}\frac{p_y}{p_x}$$

where p_x and p_y are the coordinates of the peak. All the backazimuths associated to the displayed spectra point to the crater area.

To discriminate the seismic S-phase we performed a polarization analysis using the covariance matrix technique (Jurkevics, 1988). The result of the analysis on the event 0612240 is shown in fig. 9. The S-wave has been identified with the phase coming 0.7 seconds after the P-wave onset because it has an apparent velocity which is about 1.75 times lower than the P-wave velocity and a γ angle of about 90°.

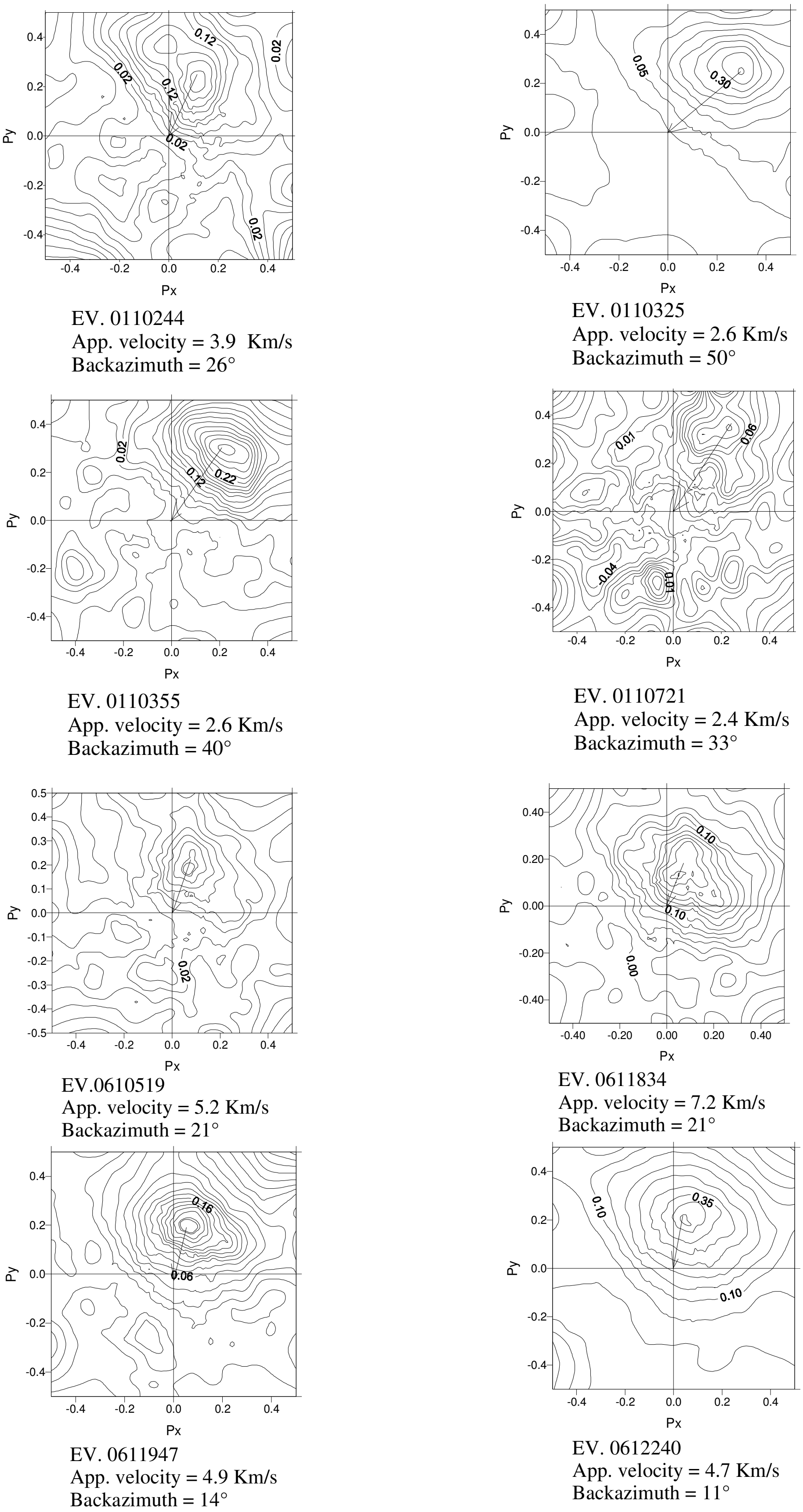

Fig. 8 - Results of the ZLCC analysis for local earthquakes belonging to the seismic swarm of January 11th (first 4 panels) and March 2nd (last 4 panels). The slowness components are reported on the x - y axes. On the contour lines the cross-correlation function assumes the same values.

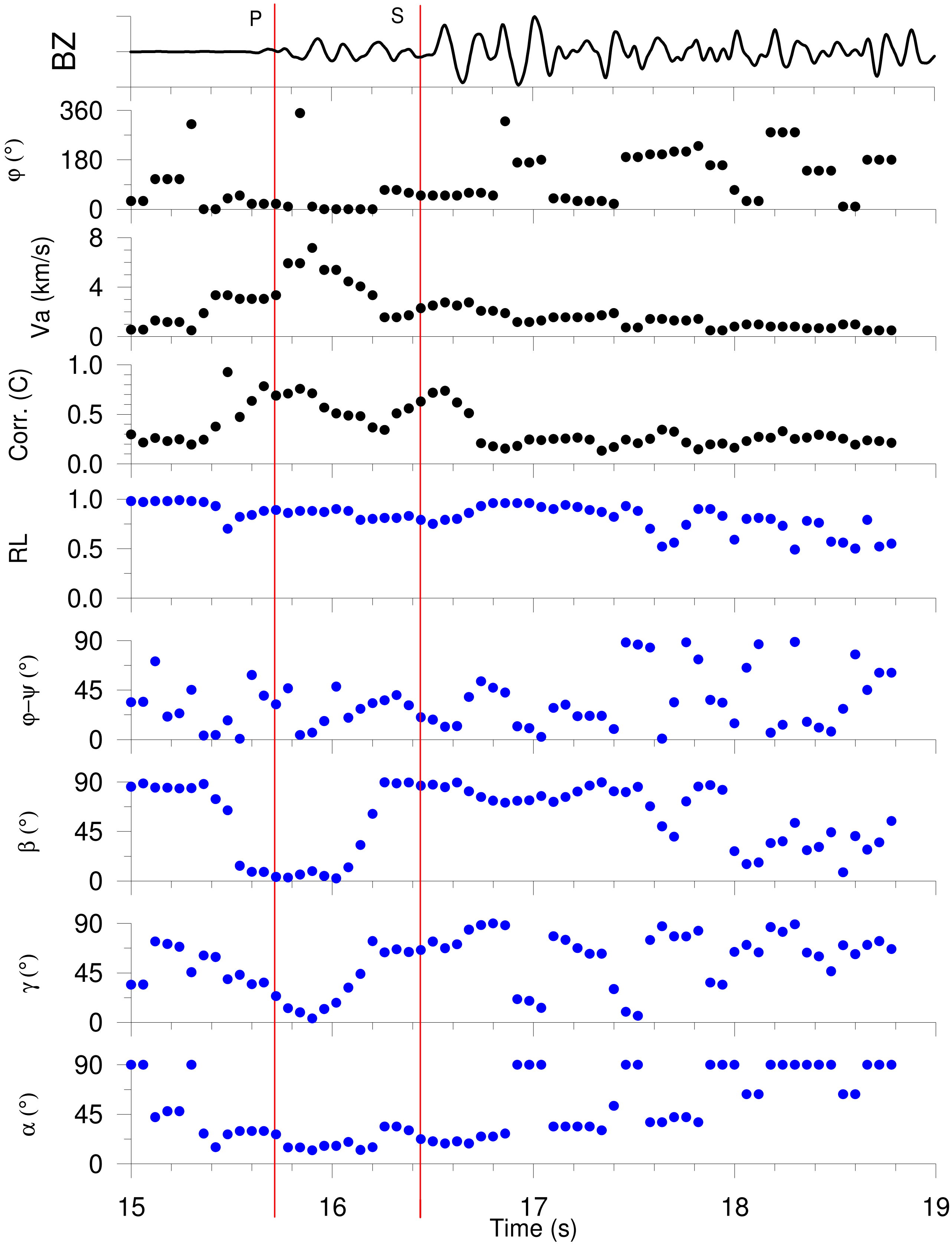

Fig. 9 - ZLCC and polarization analysis on the event 0612240. In the first panel the seismogram is represented. In the next 3 panels we plot backazimuth ϕ, apparent velocity V_a and correlation C as a function of time. In the last 5 panels we show the polarization attributes: RL is the rectilinearity, ψ is the angle between the projection of the polarization vector **p** on the surface and the North, β is the angle that **p** forms with the vertical direction, γ is the angle between **p** and the wave vector **k** and α is the angle that the **k** forms with the vertical direction (incidence angle).

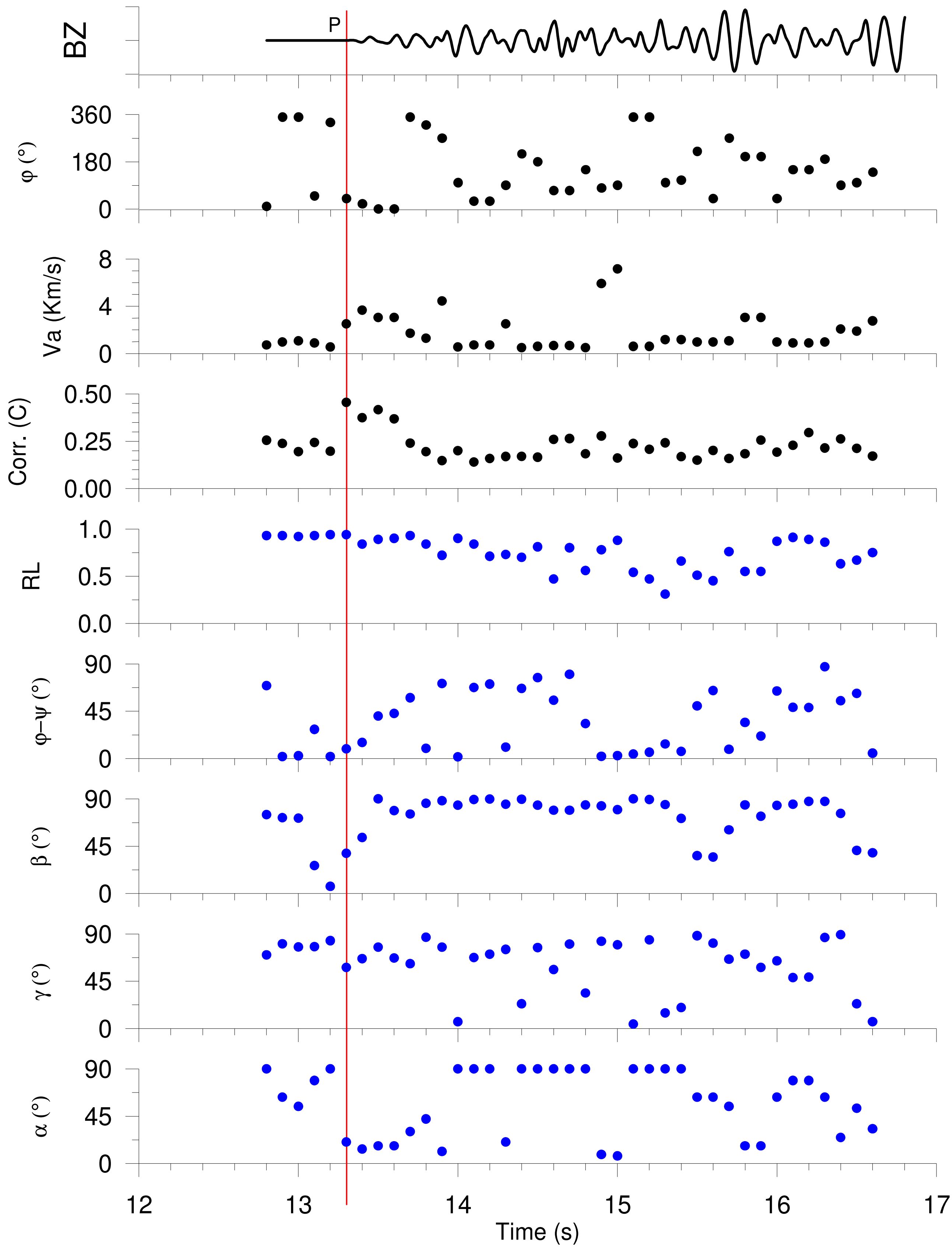

Fig. 10 - The same of fig. X for the event 0110244. The polarization analysis does not evidence the S-phase of this earthquake.

We remind that γ is the angle between the wave vector direction and the direction of the eigenvector corresponding to the highest eigenvalue of the covariance matrix. For a more detailed explanation see Del Pezzo et al. (1997) and the caption of fig. 9.

In some events the S-phase is evidenced by the polarization analysis, however there are other local earthquakes for which this phase is not clear (see for example fig. 10); this could be due to reflected and/or converted seismic phases in the wavefield which hide the S-arrival.

To constrain the depth of the earthquake sources we used a simple procedure based on a simplified 2-D ray-tracing technique and on the hypothesis that earthquake epicenters are confined in the crater area. The ray tracing technique is a modification of the Thurber (1983) procedure. It assumes that the ray path connecting source and receiver can be approximated by a second order polynomial which follows the Fermat principle. The velocity model is given on a 2-dimensional velocity grid. The search for the minimum time path is carried out with a trial and error procedure. The advantage of this approach is that the ray is expressed in an analytical form which results useful for further analyses. The computer program is reported in Appendix B.

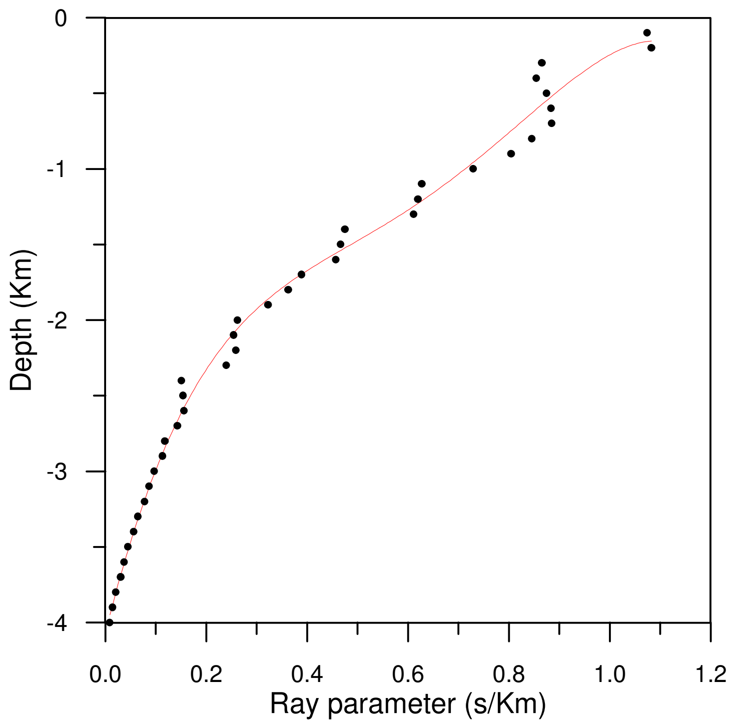

Fig. 11 - Source depth as a function of the ray parameter.

To estimate the depth of local earthquakes we proceeded in the following way: first we fixed the epicenter at the crater centre, then we estimated the polynomials associated to the rays coming at the array from sources with different depths. Furthermore we evaluated the incidence angle simply calculating the space derivative of the polynomial at the array point and hence we calculated the ray parameter (slowness at the array) for each ray. The plot of source depth as a function of the ray parameter was then fitted with a 4^{th} order polynomial, which constitutes a nomogram (fig. 11) for the determination of the source depth.

We calculated the apparent velocity applying the ZLCC technique to a time window centred around the arrival time of the P-wave onset. From the knowledge of the apparent velocity and hence of the ray parameter, we can read on the nomogram the corresponding source depth along the crater axis. Moreover if we can estimate the S-P time, we can fix the ray path length and hence locate the source position along the ray (fig 12).

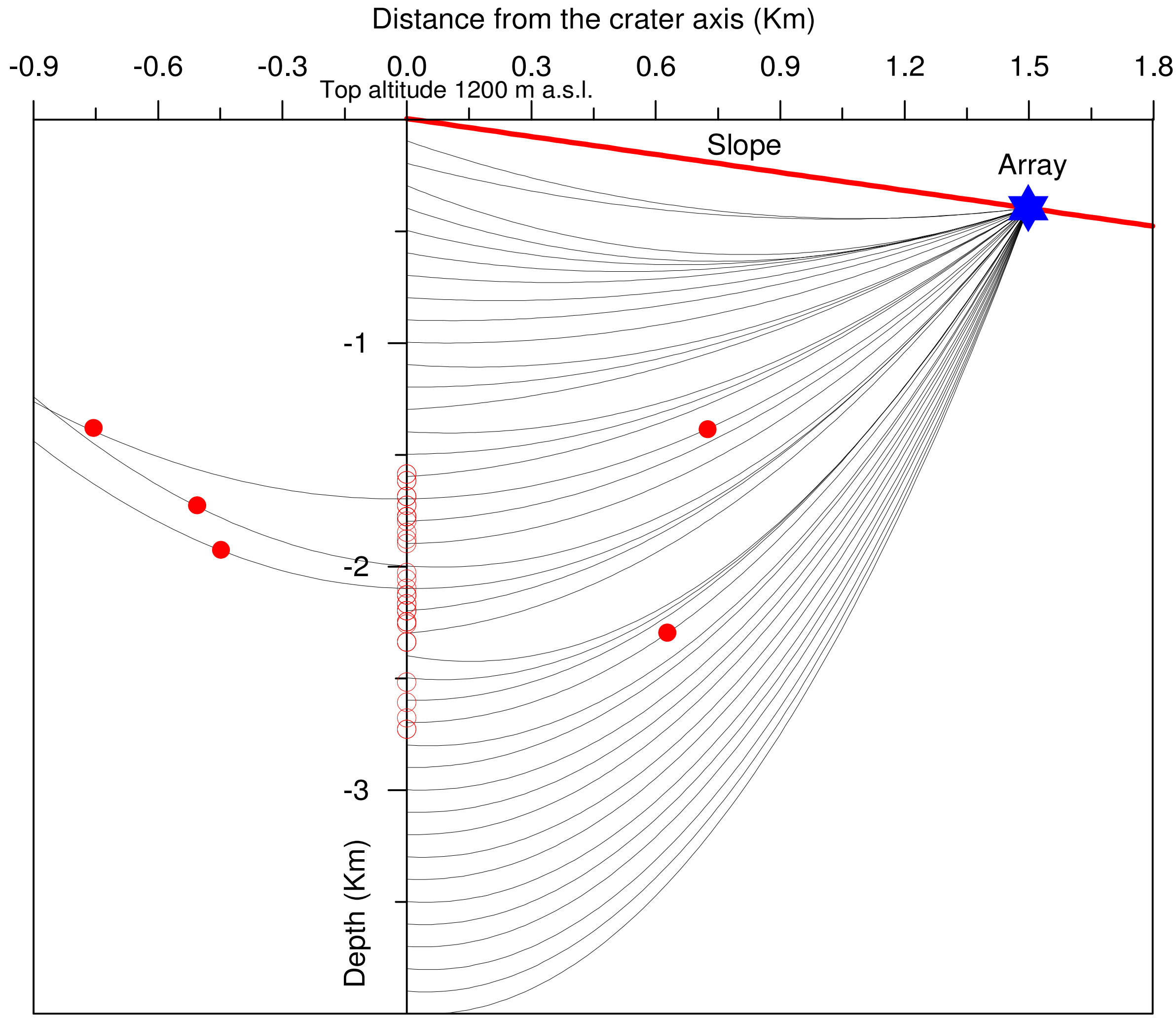

Fig. 12 - Rays obtained with the simplified 2-D ray-tracing technique. The empty circles represent the hypocenters (determined from the nomogram of fig. 11) of 40 earthquakes analysed with ZLCC technique. For 5 earthquakes it was possible to estimate the S-T time and to fix the source position along the ray (full circles).

Noise analysis

To investigate the spectral properties of the seismic noise we calculated the average spectra, which were derived for samples recorded in different days and times. An example of spectra is shown in fig. 13.

The spectra show a very clear peak at 0.5-0.7 Hz, whose amplitude does not change during day and night, two peaks at 3 and 10 Hz and other minor peaks at frequencies higher than 1-1.5 Hz. The amplitude of these last peaks depends on the day-time of the records and it is predominant in the morning hours, suggesting that these components of noise are due to the antropic activity. It is noteworthy that even though the response curve amplification at 0.5 Hz is a factor 3 lower than that at 3 Hz, the 0.5 Hz peak is clearly predominant over all the others.

MUSIC technique (Schmidt, 1981, 1986) was applied using a focusing frequency of 0.58 Hz to calculate azimuth and slowness of the sustained low frequency component. Results obtained for noise samples recorded during different day-time (fig. 14) show that the slowness is around 0.7 s/Km and the backazimuth points toward the South, in the opposite direction of the crater area. These results suggest that the low-frequency component may be due to the sea-loading in the gulf of Naples.

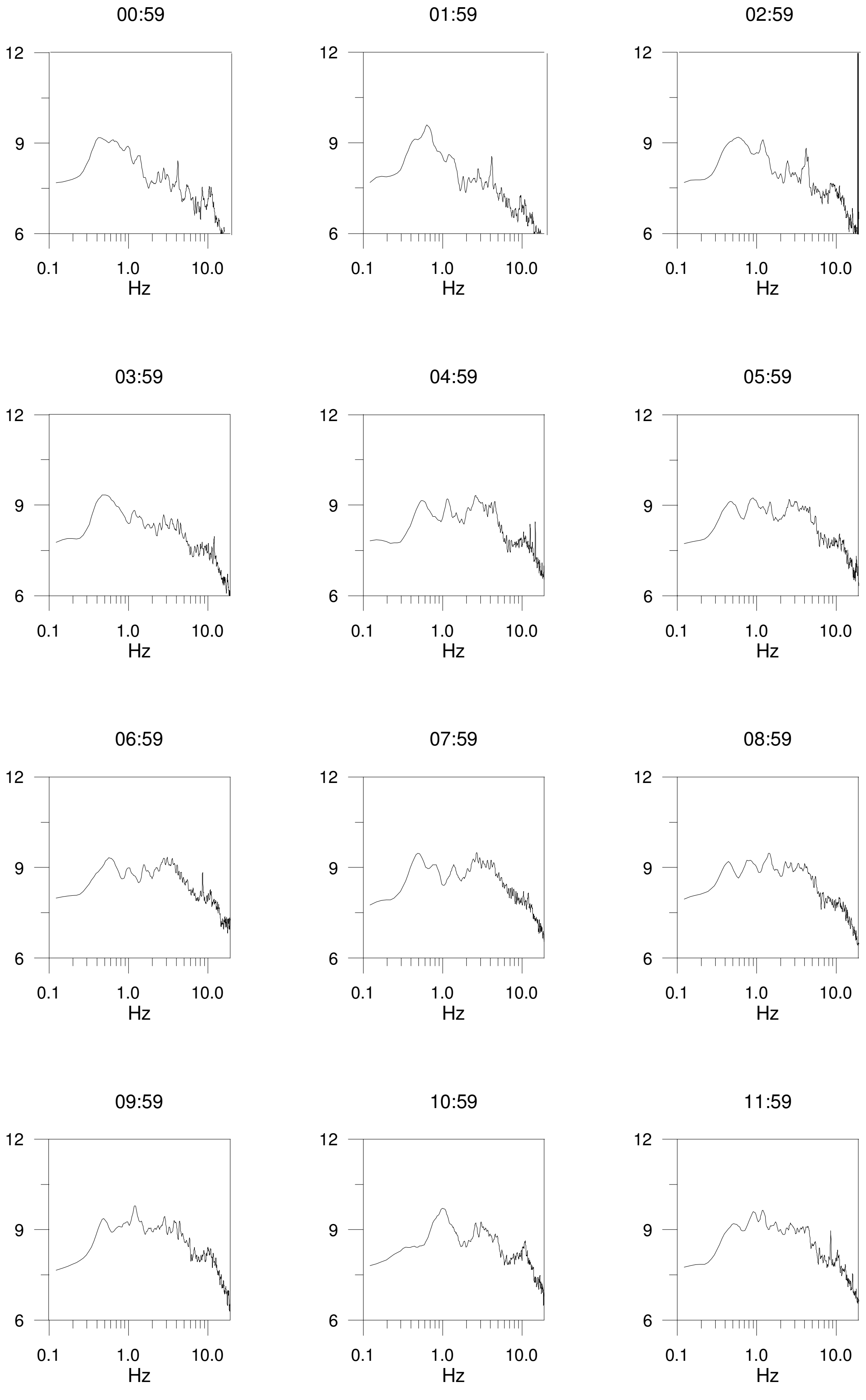

Fig. 13 - Average spectra of seismic noise recorded at different day-time on June 14th.

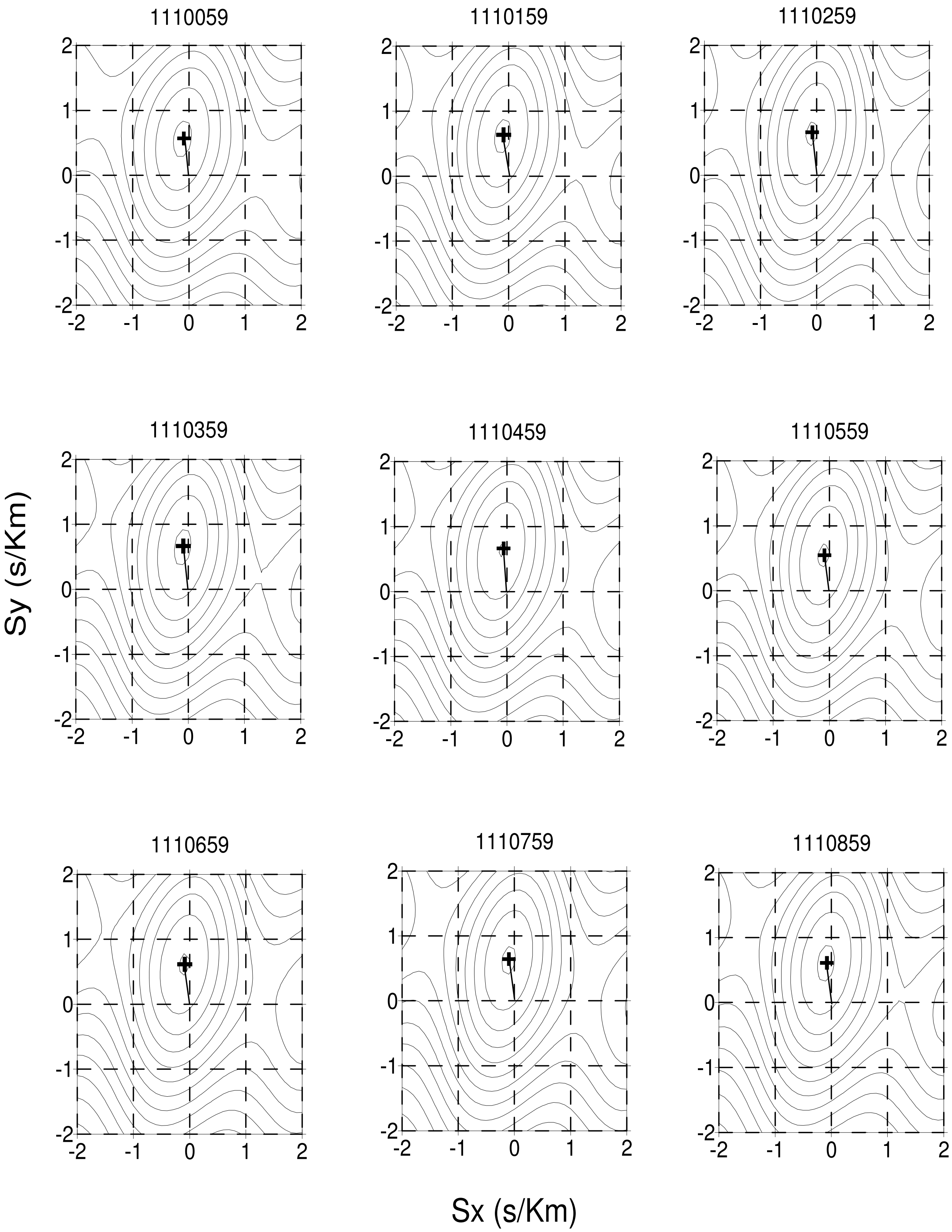

Fig. 14 - Slowness spectra obtained with MUSIC for noise samples recorded during the time interval 00:59 - 08:59 on April 21st.

Conclusions

The preliminary results can be summarised in the following statements:

1) The local earthquake source is in the direction of the crater area.
2) The use of array techniques allows the identification of the S-phase for more than the 50% of the analysed events.
3) The source location obtained from the array analysis is consistent with the location obtained using conventional techniques (Hypo71, computer program) to data recorded by the monitoring network (fig. 15).

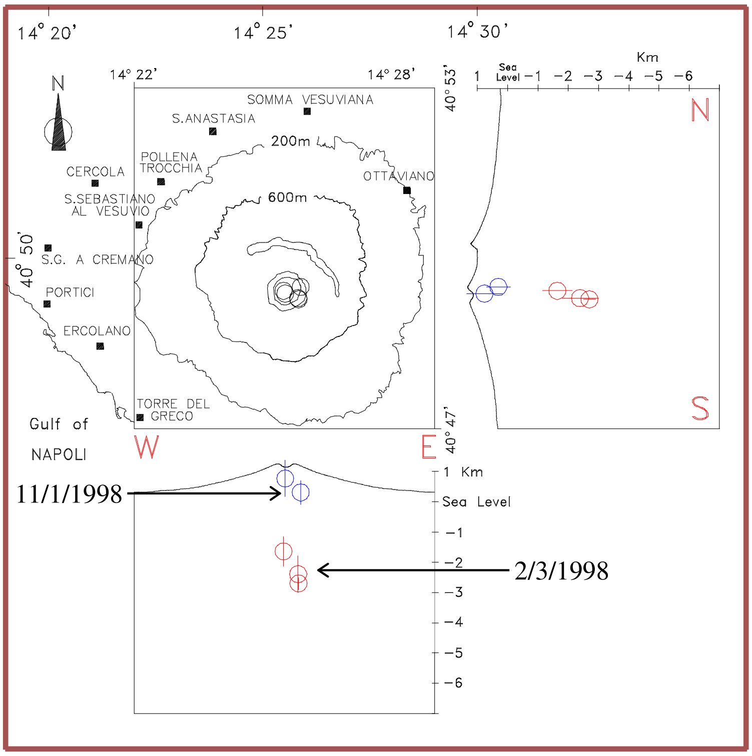

Fig. 15 - Location obtained with Hypo of some earthquakes of the seismic swarms recorded by the seismic network.

4) The source depth for the events with non-readable S-P times is constrained by the array estimate of slowness to be in the range 1.5 – 3 Km, if an epicenter in correspondence of the crater area is assumed (fig. 12).
5) A low frequency spectral peak is present in the noise wavefield. It corresponds to a coherent signal which is interpreted as related to the sea-loading in the gulf of Naples.
6) The analysis of the seismic noise shows that there is no evidence of coherent signal in the frequency band (1 – 5 Hz) characteristic of the volcanic tremor.

The results achieved during this experiment encourage to carry on further analyses on the collected data, both on local earthquakes and noise. The above results confirm that the array is an useful complementary tool for the seismic monitoring of the volcanic area. For this reason we are planning a new research project aiming both at the installation of a new multi-channel digital seismic antenna to be used for the seismic signal acquisition and at the development of real-time analysis techniques.

Acknowledgements

Part of this report is based on the Physics degree thesis of Danilo Galluzzo and Alessandra Cirillo. The instruments were assembled in the laboratory of Observatorio de Cartuja - Universidad de Granada.

References

Del Pezzo E. La Rocca M., Ibanez J., Observation of high frequency scattered waves using dense array at Teide Volcano; *B.S.S.A.*, 87,6:1637-1647, 1997.

Del Pezzo E., La Rocca M., Petrosino S., Grozea B., Maritato M., Saccorotti G., Simini M., Ibanez J., Alguacil G., Carmona E., Abril M., Almendros J., Ortiz R., Garcia A., Pingue F., Esposito T., *Twin digital short period seismic Array Experiment at Stromboli Volcano (September 1997)*; Open File Report n°1, Osservatorio Vesuviano, 1998.

Dietel C., Chouet B., Kleinman J., De Luca G., Martini M., Milana G, Power J., Harlow D., Scarpa R., Array tracking of tremor and sources at Stromboli Volcano, Italy; *U.S. Geol. Surv. Open File Report* 94-142, 1994.

Ferrazzini V., Aki K., Chouet B., Characteristic of seismic waves composing Hawaiian volacnic tremor and gas-piston events observed by a near-source array; *J. Geophys. Res.*, 96:6199-6209, 1991.

Frankel A., Hough S., Friberg P., Busby R., Observation of Loma Prieta aftershocks from a dense array in Sunnyvale, California; *B.S.S.A.*, 80:1900-1922, 1991.

Goldstein P., Chouet B., Array measurement and modeling of sources of shallow volcanic tremor at Kilauea Volcano, Hawaii; *J. Geophys. Res.*, 99:2637-2652, 1994.

Guirao, *Ph. D. Thesis*, Universidad de Granada, 1991.

Jurkevics A., Polarization Analisys of three-component array data; *B.S.S.A.*, 78, 5:1725-1743, 1988.

Olmedillas J. C., Ortiz R., Adcuisicion de datos sismicos mediante PC portatil; *Instrumentos y proceso de dato en ciencias de la tierra*, A. Garcia Edtr. Casa de los Volcanes, Cabildo Insular de Lanzarote.

Schmidt R. O., A signal subspace approach to multiple emitter location and spectral estimation; *Ph. D. Thesis, Stanford University, Palo Alto*, 1981.

Schmidt R. O., Multiple emitter location and signal parameter estimation; *IEEE Trans. Antennas Propag*., AP, 34:276-280, 1986.

Appendix A

Table A1 - List of the local earthquakes recorded at the array. The letters in the first column indicate which subarrays recorded the earthquake (for example, BCD means that all the 3 subarrays triggered). The X in the 5th column (N) means that the event was recorded by the seismic network too.

Event	Day	GMT	N	Event	Day	GMT	N	Event	Day	GMT	N
3101455 B	06/11/97	14:55		3231336 C	19/11/97	13:36		3381604 BC	04/12/97	16:04	
3110014 BD	07/11/97	00:14		3241624 BCD	20/11/97	16:24	X	3381608 B	04/12/97	16:08	
3110029 BD	07/11/97	00:29		3250143 BCD	21/11/97	01:43		3390202 BC	05/12/97	02:02	
3110205 B	07/11/97	02:05	X	3250347 BCD	21/11/97	03:47		3390343 B	05/12/97	03:43	
3111434 C	07/11/97	14:34		3260906 BCD	22/11/97	09:06		3390944 BC	05/12/97	09:44	
3112115 BCD	07/11/97	21:15		3261951 BCD	22/11/97	19:51		3391121 BCD	05/12/97	11:21	X
3120234 C	08/11/97	02:34		3282100 BCD	24/11/97	21:00	X	3391130 C	05/12/97	11:30	
3120945 C	08/11/97	09:45		3290821 BCD	25/11/97	08:21	X	3391132 BC	05/12/97	11:32	X
3121511 C	08/11/97	15:11	X	3291024 BCD	25/11/97	10:24	X	3391711 C	05/12/97	17:11	
3130007 C	09/11/97	00:07		3300444 BCD	26/11/97	04:44		3410155 C	07/12/97	01:55	
3130755 C	09/11/97	07:55	X	3300910 BCD	26/11/97	09:10		3420600 C	08/12/97	06:00	
3131150 D	09/11/97	11:50		3301934 BCD	26/11/97	19:34		3421733 BC	08/12/97	17:33	
3131830 C	09/11/97	18:30		3302224 BCD	26/11/97	22:24		3430424 BC	09/12/97	04:24	
3132044 C	09/11/97	20:44	X	3311000 C	27/11/97	10:00		3432145 BC	09/12/97	21:45	
3140140 C	10/11/97	01:40	X	3311347 BCD	27/11/97	13:47		3432221 BC	09/12/97	22:21	
3140616 C	10/11/97	06:16		3311810 BCD	27/11/97	18:10		3432259 B	09/12/97	22:59	
3140748 C	10/11/97	07:48	X	3320025 BCD	28/11/97	00:25		3440047 BC	10/12/97	00:47	
3140817 C	10/11/97	08:17		3320035 BCD	28/11/97	00:35		3440112 BC	10/12/97	01:12	
3141000 C	10/11/97	10:00	X	3320226 BCD	28/11/97	02:26		3440209 BC	10/12/97	02:09	
3141908 CD	10/11/97	19:08		3321901 BCD	28/11/97	19:01		3440248 BC	10/12/97	02:48	
3141910 BCD	10/11/97	19:10		3330231 BCD	29/11/97	02:31		3440618 BC	10/12/97	06:18	
3141927 D	10/11/97	19:27		3331424 BCD	29/11/97	14:24		3450652 C	11/12/97	06:52	
3150206 BCD	11/11/97	02:06		3340716 BC	30/11/97	07:16		3451425 BC	11/12/97	14:25	
3150707 B	11/11/97	07:07		3341233 BC	30/11/97	12:33		3451537 BCD	11/12/97	15:37	
3151744 B	11/11/97	17:44		3341234BC	30/11/97	12:34		3471029 C	13/12/97	10:29	
3151910 BD	11/11/97	19:10		3341351 C	30/11/97	13:51		3490001 BCD	15/12/97	00:01	X
3162356 C	12/11/97	23:56		3341522 BCD	30/11/97	15:22		3490502 CD	15/12/97	05:02	
3162358 C	13/11/97	23:58		3341702 BCD	30/11/97	17:02		3490956 CD	15/12/97	09:56	
3170007 BC	13/11/97	00:07		3342008 CD	30/11/97	20:08		3491831 B	15/12/97	18:32	
3170011 C	13/11/97	00:11		3342246 C	30/11/97	22:46		3492009 BCD	15/12/97	20:09	
3170153 C	13/11/97	01:53		3350342 CD	01/12/97	03:42		3492013 BCD	15/12/97	20:13	
3170204 C	13/11/97	02:04		3350900 CD	01/12/97	09:00		3492346 BCD	15/12/97	23:46	
3170206 C	13/11/97	02:06		3351252 BCD	01/12/97	12:52		3500816 BCD	16/12/97	08:16	
3170208 C	13/11/97	02:08		3351608 BCD	01/12/97	16:08		3502025 BCD	16/12/97	20:25	X
3170719 C	13/11/97	07:19		3361538C	02/12/97	15:38		3510432 BCD	17/12/97	04:32	
3170733 C	13/11/97	07:33		3361600 CD	02/12/97	16:00		3550157 B	21/12/97	01:57	
3172254 B	13/11/97	22:54		3361617 BCD	02/12/97	16:17		3550414 BCD	21/12/97	04:14	
3172257 BD	13/11/97	22:57		3362218 BCD	02/12/97	22:18	X	3551042 BCD	21/12/97	10:42	
3172309 BD	13/11/97	23:09		3370226 BCD	03/12/97	02:26		3551045 CD	21/12/97	10:45	
3172312 BD	13/11/97	23:12		3370752 BCD	03/12/97	07:52		3551805 C	21/12/97	18:05	
3172315 BD	13/11/97	23:15		3371148 BD	03/12/97	11:48		3551808 BC	21/12/97	18:08	
3180821 D	14/11/97	08:21		3372015 BCD	03/12/97	20:15		3551830C	21/12/97	18:30	
3200656 BCD	16/11/97	06:56		3372049 C	03/12/97	20:49		3551833 BCD	21/12/97	18:33	
3211317 C	17/11/97	13:17		3380031 B	04/12/97	00:31		3552122 BCD	21/12/97	21:22	
3220127 BC	18/11/97	01:27		3380302 BC	04/12/97	03:02		3560232 BCD	22/12/97	02:32	
3220817 BCD	18/11/97	08:17		3380306 BC	04/12/97	03:06		3560234 BD	22/12/97	02:34	
3221032 BC	18/11/97	10:32		3380404 BC	04/12/97	04:04		3561829 BCD	22/12/97	18:29	
3221833 C	18/11/97	18:33		3380536 BC	04/12/97	05:36		3562330 BCD	22/12/97	23:30	

Event	Day	GMT	N		Event	Day	GMT	N		Event	Day	GMT	N
3562332 B	22/12/97	23:32			0110248 CD	11/01/98	02:48	X		0282157 BCD	28/01/98	21:57	X
3591654 BD	25/12/97	16:54			0110249 C	11/01/98	02:49	X		0290133 BCD	29/01/98	01:33	X
3591701 BCD	25/12/97	17:01			0110250 BD	11/01/98	02:50	X		0300052 BCD	30/01/98	00:52	X
3592059 D	25/12/97	20:59			0110252 BCD	11/01/98	02:52	X		0300347 BCD	30/01/98	03:47	
3601612 BCD	26/12/97	16:12			0110253 CD	11/01/98	02:53	X		0302149 BCD	30/01/98	21:49	X
3602146 BCD	26/12/97	21:46			0110255 CD	11/01/98	02:55	X		0310049 BCD	31/01/98	00:49	X
3611544 B	27/12/97	15:44			0110256 B	11/01/98	02:56	X		0310051 C	31/01/98	00:51	X
3611718 B	27/12/97	17:18			0110258 CD	11/01/98	02:58	X		0310053 BD	31/01/98	00:53	
3620653 BCD	28/12/97	06:53			0110259 B	11/01/98	02:59	X		0311007 BCD	31/01/98	10:07	
3622311 BCD	28/12/97	23:11			0110301 CD	11/01/98	03:01			0341846 BCD	03/02/98	18:46	
3632204 BC	29/12/97	22:04			0110304 BCD	11/01/98	03:04	X		0351654 BCD	04/02/98	16:54	
3641732 BC	30/12/97	17:32			0110307 CD	11/01/98	03:07	X		0361823 BCD	05/02/98	18:23	
0010433 BCD	01/01/98	04:33			0110311 CD	11/01/98	03:11	X		0380104 BCD	07/02/98	01:04	X
0010922 BC	01/01/98	09:22			0110312 BC	11/01/98	03:12	X		0391611 BCD	08/02/98	16:11	X
0011059 BCD	01/01/98	10:59			0110314 BCD	11/01/98	03:14	X		0391629 BCD	08/02/98	16:29	X
0012134 BCD	01/01/98	21:34			0110316 BCD	11/01/98	03:16	X		0410138 BCD	10/02/98	01:38	X
0012137 BCD	01/01/98	21:37			0110325 BCD	11/01/98	03:25	X		0410834 BCD	10/02/98	08:34	
0012230 C	01/01/98	22:30	X		0110341 BCD	11/01/98	03:41	X		0412041 BCD	10/02/98	20:41	X
0012231 BD	01/01/98	22:31			0110347 BCD	11/01/98	03:47	X		0440404 BCD	13/02/98	04:04	X
0020059 BC	02/01/98	00:59			0110348 D	11/01/98	03:48	X		0460703 BC	15/02/98	07:03	X
0021821 BCD	02/01/98	18:21			0110355 BCD	11/01/98	03:55	X		0491242 BCD	18/02/98	12:42	X
0030328 BC	03/01/98	03:28			0110359 C	11/01/98	03:59			0491708 BCD	18/02/98	17:08	X
0030343 B	03/01/98	03:43			0110402 CD	11/01/98	04:02	X		0501617 D	19/02/98	16:17	X
0030727 BD	03/01/98	07:27			0110542 BCD	11/01/98	05:42	X		0502221 D	19/02/98	22:21	X
0031255 BCD	03/01/98	12:55			0110552 BCD	11/01/98	05:52	X		0530034 BCD	22/02/98	00:34	
0031654 BCD	03/01/98	16:54	X		0110628 CD	11/01/98	06:28	X		0541448 BCD	23/02/98	14:48	
0041623 BCD	04/01/98	16:23	X		0110630 BC	11/01/98	06:30	X		0541732 BCD	23/02/98	17:32	
0050340 C	05/01/98	03:40	X		0110635 D	11/01/98	06:35			0541933 BCD	23/02/98	19:33	
0051217 BCD	05/01/98	12:17	X		0110639 BCD	11/01/98	06:39			0550431 C	24/02/98	04:31	
0051218 BCD	05/01/98	12:18	X		0110646 BCD	11/01/98	06:46	X		0550609 C	24/02/98	06:09	
0060610 D	06/01/98	06:10	X		0110706 D	11/01/98	07:06			0550613 CD	24/02/98	06:13	
0061307 BCD	06/01/98	13:07	X		0110719 BCD	11/01/98	07:19	X		0551923 BCD	24/02/98	19:23	
0082341 CD	08/01/98	23:41			0110721 BCD	11/01/98	07:21	X		0571453 BCD	26/02/98	14:53	
0091723 BCD	09/01/98	17:23			0110747 BCD	11/01/98	07:47	X		0580342 BCD	27/02/98	03:42	X
0100046 BCD	10/01/98	00:46	X		0110958 BCD	11/01/98	09:58	X		0580752 BCD	27/02/98	07:52	X
0100333 CD	10/01/98	03:33			0111042 BCD	11/01/98	10:42	X		0581144 CD	27/02/98	11:44	
0100414 BCD	10/01/98	04:14			0111108 BCD	11/01/98	11:08	X		0582018 BCD	27/02/98	20:18	X
0100418 BCD	10/01/98	04:18	X		0111357 BCD	11/01/98	13:57	X		0582022 BCD	27/02/98	20:22	X
0101114 BCD	10/01/98	11:14			0120157 BCD	12/01/98	01:57			0590216 BCD	28/02/98	02:16	X
0101439 BCD	10/01/98	14:39			0120301 BCD	12/01/98	03:01	X		0590539 BCD	28/02/98	05:39	X
0101612 BCD	10/01/98	16:12	X		0120741 BCD	12/01/98	07:41			0590629 D	28/02/98	06:29	
0101618 BCD	10/01/98	16:18	X		0121055 BCD	12/01/98	10:55			0590820 BCD	28/02/98	08:20	X
0101622 BCD	10/01/98	16:22	X		0121128 BCD	12/01/98	11:28	X		0591844 BCD	28/02/98	18:44	X
0101627 BCD	10/01/98	16:27			0121717 BCD	12/01/98	17:17	X		0592114 BCD	28/02/98	21:14	X
0101631 BCD	10/01/98	16:31			0122310 C	12/01/98	23:10			0592145 BCD	28/02/98	21:45	X
0101638 BCD	10/01/98	16:38			0142313 D	14/01/98	23:13			0600026 BCD	01/03/98	00:26	X
0101957 BCD	10/01/98	19:57	X		0142314 BC	14/01/98	23:14			0600453 BCD	01/03/98	04:53	X
0102009 BCD	10/01/98	20:09	X		0181101 CD	18/01/98	11:01	X		0601846 BCD	01/03/98	18:46	X
0110035 BCD	11/01/98	00:35	X		0181206 BCD	18/01/98	12:06	X		0602148 BCD	01/03/98	21:48	X
0110103 BCD	11/01/98	01:03			0211150 BCD	21/01/98	11:50			0610117 CD	02/03/98	01:17	
0110147 BCD	11/01/98	01:47	X		0211202 CD	21/01/98	12:02	X		0610158 CD	02/03/98	01:58	
0110235 CD	11/01/98	02:35			0222225 C	22/01/98	22:25			0610519 BCD	02/03/98	05:19	X
0110241 BCD	11/01/98	02:41	X		0240351 CD	24/01/98	03:51	X		0610555CD	02/03/98	05:55	X
0110242 CD	11/01/98	02:42	X		0272108 BCD	27/01/98	21:08			0610649 BCD	02/03/98	06:49	X
0110244 BCD	11/01/98	02:44	X		0280551 C	28/01/98	05:51			0611834 BCD	02/03/98	18:34	X
0110245 CD	11/01/98	02:45	X		0281220 D	28/01/98	12:20	X		0611933 BCD	02/03/98	19:33	X
0110247 B	11/01/98	02:47	X		0281221 CD	28/01/98	12:21	X		0611937 BCD	02/03/98	19:37	X

Event	Day	GMT	N		Event	Day	GMT	N		Event	Day	GMT	N
0611947 BCD	02/03/98	19:47	X		0970929 BCD	07/04/98	09:29			1342218 BD	14/05/98	22:18	X
0612132 CD	02/03/98	21:32	X		0982235 BCD	08/04/98	22:35			1370046 BD	17/05/98	00:46	
0612218 BCD	02/03/98	22:18	X		1020134 BCD	12/04/98	01:34	X		1370051 BD	17/05/98	00:51	
0612240 BCD	02/03/98	22:40	X		1020248 BCD	12/04/98	02:48			1372125 D	17/05/98	21:25	
0612243 BCD	02/03/98	22:43	X		1040432 BCD	14/04/98	04:32			1372138 C	17/05/98	21:38	
0612251 BCD	02/03/98	22:51			1040439 BCD	14/04/98	04:39			1392044 D	19/05/98	20:44	X
0620154 BCD	03/03/98	01:54	X		1050943 BCD	15/04/98	09:43	X		1392049 D	19/05/98	20:49	X
0620314 BCD	03/03/98	03:14	X		1071625 BCD	17/04/98	16:25	X		1400853 BCD	20/05/98	08:53	X
0620549 BCD	03/03/98	05:49	X		1080528 CD	18/04/98	05:28			1401508 BCD	20/05/98	15:08	X
0620708 BCD	03/03/98	07:08	X		1081604 BC	18/04/98	16:04			1410035 CD	21/05/98	00:35	
0621220 BCD	03/03/98	12:20	X		1091213 BCD	19/04/98	12:13	X		1440152 BCD	24/05/98	01:52	
0621308 CD	03/03/98	13:08	X		1091423 BCD	19/04/98	14:23	X		1440744 D	24/05/98	07:44	X
0621309 B	03/03/98	13:09	X		1100652 BD	20/04/98	06:52	X		1442206 BCD	24/05/98	22:06	X
0621310 BC	03/03/98	13:10	X		1101053 D	20/04/98	10:53			1450656 BCD	25/05/98	06:56	
0621319 BCD	03/03/98	13:19	X		1110920 BCD	21/04/98	09:20			1451050 BCD	25/05/98	10:50	
0630036 BCD	04/03/98	00:36	X		1120210 BCD	22/04/98	02:10	X		1451051 BCD	25/05/98	10:51	
0631538 BCD	04/03/98	15:38	X		1120543 BCD	22/04/98	05:43	X		1451934 C	25/05/98	19:34	
0632135 BCD	04/03/98	21:35	X		1130017 BCD	23/04/98	00:17			1451955 BCD	25/05/98	19:55	X
0640216 BCD	05/03/98	02:16	X		1130020 BC	23/04/98	00:20			1472224 BCD	27/05/98	22:24	
0650337 BCD	06/03/98	03:37	X		1130023 BCD	23/04/98	00:23			1480514 BCD	28/05/98	05:14	X
0651458 BCD	06/03/98	14:58			1130057 BCD	23/04/98	00:57			1502030 BCD	30/05/98	20:30	X
0660042 BCD	07/03/98	00:42	X		1130109 C	23/04/98	01:09			1502132 BCD	30/05/98	21:32	X
0672020 BC	08/03/98	20:20	X		1130342 BCD	23/04/98	03:42			1510304 BCD	31/05/98	03:04	X
0721820 BCD	13/03/98	18:20	X		1131950 BCD	23/04/98	19:50	X		1511023 BCD	31/05/98	10:23	X
0771118 BD	18/03/98	11:18	X		1150745 BCD	25/04/98	07:45			1511427 BCD	31/05/98	14:27	X
0771155 BD	18/03/98	11:55	X		1160534 BCD	26/04/98	05:34	X		1520834 BCD	01/06/98	08:34	X
0812036 BCD	22/03/98	20:36	X		1172128 BC	27/04/98	21:28			1531904 BCD	02/06/98	19:04	X
0812052 CD	22/03/98	20:52	X		1172129 D	27/04/98	21:29			1542322 BCD	03/06/98	23:22	X
0832125 BC	24/03/98	21:25			1190855 B	29/04/98	08:55			1551659 BCD	04/06/98	16:59	X
0890229 BCD	30/03/98	02:29	X		1192134 BCD	29/04/98	21:34			1560000 CD	05/06/98	00:00	X
0892235 BCD	30/03/98	22:35	X		1200454 BCD	30/04/98	04:54	X		1560958 BCD	05/06/98	09:58	X
0901655 C	31/03/98	16:55			1212215 BCD	01/05/98	22:15			1560959 BC	05/06/98	09:59	X
0910508 BCD	01/04/98	05:08			1220011 BCD	02/05/98	00:11			1561005 BCD	05/06/98	10:05	X
0910914 C	01/04/98	09:14			1221313 BCD	02/05/98	13:13			1561156 BCD	05/06/98	11:56	
0912344 BCD	01/04/98	23:44	X		1230033 BCD	03/05/98	00:33			1570426 BCD	06/06/98	04:26	
0920841 BCD	02/04/98	08:41	X		1230116 BC	03/05/98	01:16	X		1570701 BCD	06/06/98	07:01	X
0921325 BD	02/04/98	13:25			1230153 BCD	03/05/98	01:53			1581355 BCD	07/06/98	13:55	X
0921454 BCD	02/04/98	14:54	X		1231612 BD	03/05/98	16:12	X		1581723 BCD	07/06/98	17:23	
0931809 B	03/04/98	18:09			1240248 B	04/05/98	02:48			1590707 BCD	08/06/98	07:07	
0940707 BCD	04/04/98	07:07	X		1240249 CD	04/05/98	02:49	X		1592123 BCD	08/06/98	21:23	
0940712 D	04/04/98	07:12	X		1240737 BCD	04/05/98	07:37	X		1602013 BC	09/06/98	20:13	
0940714 BC	04/04/98	07:14	X		1242102 BCD	04/05/98	21:02	X		1610110 BC	10/06/98	01:10	
0940802 BCD	04/04/98	08:02	X		1302059 BD	10/05/98	20:59	X		1611736 BC	10/06/98	17:36	X
0940918 BCD	04/04/98	09:18	X		1302204 BD	10/05/98	22:04	X		1611739 BC	10/06/98	17:39	X
0961010 BC	06/04/98	10:10	X		1322019 BD	12/05/98	20:19	X		1611748 BC	10/06/98	17:48	X
0962355 BCD	06/04/98	23:55			1341629 BCD	14/05/98	16:29	X		1611831 BC	10/06/98	18:31	X

Table. A2 - List of the regional earthquakes recorded both at the array and at the seismic network

Event	Date	GMT	Location
3221308 C	18/11/97	13:08	Greece M=6.1
3221315 BC	18/11/97	13:15	Greece
3221501 C	18/11/97	15:01	Greece
3221524 BC	18/11/97	15:24	Greece
3221805 B	18/11/97	18:05	Greece
3281904 BCD	24/11/97	19:04	Sannio-Matese M=3.8
3290137 BCD	25/11/97	01:37	Sannio-Matese M=3.5
3442109 BC	10/12/97	21:09	Sannio-Matese
0100435 CD	10/01/98	04:35	Regional earthquake
0101923 BCD	10/01/98	19:23	Regional earthquake
0262317 BCD	26/01/98	23:17	Regional earthquake M=3.7
0660327 CD	07/03/98	03:27	Regional earthquake
0851626 BCD	26/03/98	16:26	Umbria-Marche
0972137 BCD	07/04/98	21:37	Lavello-Venosa M=3.9
1122339 BCD	22/04/98	23:39	Cervinara Valle Caudina M=3.0
1190332 BC	29/04/98	03:32	Greece M=5.4
1381719 BCD	18/05/98	17:19	Tyrrhenian Sea

.**Table A3 -** List of the artificial explosions recorded both at the array and at the seismic network

Event	Date	GMT	Type
3580157 BCD	24/12/97	01:57	Probable artificial explosion
3591736 BCD	25/12/97	17:36	Probable artificial explosion
3591756 BC	25/12/97	17:56	Probable artificial explosion
0461801 BC	15/02/98	18:01	Artificial explosion
0461829 BC	15/02/98	18:29	Artificial explosion
0491124 BCD	18/02/98	11:24	Artificial explosion
0502313 D	19/02/98	23:13	Artificial explosion
0590342 BCD	28/02/98	03:42	Artificial explosion
1121442 BCD	22/04/98	14:42	Under-sea explosion

Table A4 - List of the 215 seismic noise samples which were recorded programming time windows of 120 s. For each programmed recording, we report day and time of the first noise sample, day and time of the last sample, the number of time windows (the frequency of the programmed windows was 1/hour) and the configuration of the array..

Day and starting time	Day and ending time	# of programmed windows	Configuration
17/04/98 17:59	18/04/98 16:59	24	A
20/04/98 17:59	21/04/98 16:59	24	A
24/04/98 17:59	25/04/98 16:59	24	A
27/04/98 17:59	28/04/98 16:59	24	A
30/04/98 17:59	01/05/98 16:59	24	A
03/06/98 17:59	04/06/98 16:59	23	A
13/06/98 23:59	15/06/98 22:59	72	B

Appendix B

We report the list of 2-D ray tracing program.

```
DECLARE FUNCTION ray! (a!, b!, c!, x!)
DECLARE SUB interpol (ncolonne, nrighe, xval!, zval!, vinterp!)
DIM trav(2000), a222(2000), a111(2000)
' programma di ray tracing su griglia
INPUT "nome file modello di velocita", nome$
INPUT "nome file uscita", nime$
INPUT "coordinate stazione"; xr, zr
INPUT "coordinate  evento,z negativa"; xs, zs
INPUT "numero passi deltax", nstep
OPEN nome$ FOR INPUT AS #1
OPEN nime$ FOR OUTPUT AS #3
PRINT #3, xr, zr
PRINT #3, xs, zs
'legge la griglia di velocit…
INPUT #1, ncolonne, nrighe
DIM x(ncolonne, nrighe), z(ncolonne, nrighe), v(ncolonne, nrighe)
FOR i = 1 TO ncolonne
FOR j = 1 TO nrighe
INPUT #1, x(i, j), z(i, j), v(i, j)
'PRINT x(i, j), z(i, j), v(i, j), i, j
NEXT j
NEXT i
'----------------------------------------------------------
' si opera una trasformazione di coordinate per porre a zero
'la coordinata xs
' PRINT "modello corretto"
FOR i = 1 TO ncolonne
FOR j = 1 TO nrighe
x(i, j) = x(i, j) - xs
' PRINT x(i, j), z(i, j), v(i, j), i, j
NEXT j
 NEXT i
xr = xr - xs
 xs = 0
'----------------------------------------------------------------
' calcola il coeff. ang della retta stazione sorgente
a1 = (zr - zs) / xr
alfa1 = ATN(a1)
deltax = xr / nstep
PRINT "a1,alfa1,deltax", a1, alfa1, deltax
'alfa1 in radianti
pig = 3.1415
IF a1 >= 0 THEN
alfaincrem = 2 * pig / 100
END IF
IF a1 < 0 THEN
```

```
alfaincrem = 2 * pig / 360
END IF
index = 0
'-----------------------------------
'-------------------------------------
121 alfa1 = alfa1 - alfaincrem
index = index + 1
PRINT "nuova iterazione,index# ", index
IF alfa1 < (-pig / 2) + ABS(3 * alfaincrem) THEN GOTO 2332
a11 = TAN(alfa1)
' la seguente formula Š stata modificata rispetto alla versione precedente
' RAYT2D2: al posto di xr ora compaiono le differenze (xr - xs)
a22 = (zr - zs - a11 * (xr - xs)) / (xr - xs) ^ 2
PRINT "a11,a22", a11, a22
'il polinomio sara' z=zs+a11*x+a22*x^2 la funzione e' ray(a,b,c,x)
'che lo definisce con zs=a,a11=b,a22=c
sum = 0
FOR i = 1 TO nstep
  zray = ray(zs, a11, a22, (i - 1) * deltax)
  deltaz = ray(zs, a11, a22, i * deltax) - ray(zs, a11, a22, (i - 1) * deltax)
  CALL interpol(ncolonne, nrighe, (i - 1) * deltax, zray, vel)
  PRINT "velocita'", vel, "iterazione", i
  p = 1 / vel
  deltas = SQR(deltax ^ 2 + deltaz ^ 2)
  sum = sum + p * deltas
NEXT i
traveltime = sum
PRINT "traveltime", traveltime
trav(index) = traveltime
a111(index) = a11
a222(index) = a22
PRINT #3, zs, a11, a22, traveltime
 GOTO 121
2332  mintrav = trav(1)
    indice = 0
FOR k = 1 TO index - 1
        IF trav(k) <= mintrav THEN
        mintrav = trav(k)
        indice = k
        END IF
        NEXT k
        PRINT "zs,a11,a22,trav time", zs, a111(indice), a222(indice), trav(indice)
 END

SUB interpol (ncolonne, nrighe, xval, zval, vinterp)
SHARED x(), z(), v()
'PRINT "xval,zval", xval, zval
xmax = x(ncolonne, nrighe)
xmin = x(1, 1)
zmax = z(1, 1)
```

```
zmin = z(ncolonne, nrighe)
'PRINT "xmax,xmin,zmax,zmin", xmax, xmin, zmax, zmin
FOR i = 1 TO ncolonne
FOR j = 1 TO nrighe
  IF x(i, j) < xval THEN
                 IF x(i, j) >= xmin THEN
                 xmin = x(i, j)
                 icol = i
                 END IF
   END IF
   NEXT j
   NEXT i
   FOR j = 1 TO nrighe
   IF z(icol, j) > zval THEN
                 IF z(icol, j) <= zmax THEN
                  zmax = z(icol, j)
                 jrig = j
                 END IF
   END IF
   NEXT j
IF icol = 0 THEN icol = 1
IF jrig = 0 THEN jrig = 1
IF icol >= ncolonne THEN icol = ncolonne - 1
IF jrig >= nrighe THEN jrig = nrighe - 1
'PRINT "icol, cioe' lindice di colonna prima del valore", icol
'PRINT "jrig, cioe' l'indice di riga subito prima del valore", jrig
' ora la interpolazione avviene tra v(icol,jrig),v(icol,jrig+1),v(icol+1,jrig),
'e v(icol+1,jrig+1)  con una media pesata per le distanze inverse
dist1 = SQR((x(icol, jrig) - xval) ^ 2 + (z(icol, jrig) - zval) ^ 2)
dist2 = SQR((x(icol, jrig + 1) - xval) ^ 2 + (z(icol, jrig + 1) - zval) ^ 2)
dist3 = SQR((x(icol + 1, jrig) - xval) ^ 2 + (z(icol + 1, jrig) - zval) ^ 2)
dist4 = SQR((x(icol + 1, jrig + 1) - xval) ^ 2 + (z(icol + 1, jrig + 1) - zval) ^ 2)
IF dist1 < 10 ^ -6 THEN dist1 = .0001
IF dist2 < 10 ^ -6 THEN dist2 = .0001
IF dist3 < 10 ^ -6 THEN dist3 = .0001
IF dist4 < 10 ^ -6 THEN dist4 = .0001
denom = (1 / dist1) + (1 / dist2) + (1 / dist3) + (1 / dist4)
'PRINT "v(icol, jrig)", v(icol, jrig)
'PRINT "v(icol + 1, jrig)", v(icol + 1, jrig)
vinterp = (v(icol, jrig) / dist1) + (v(icol, jrig + 1) / dist2) + (v(icol + 1, jrig) / dist3) + (v(icol +
1, jrig + 1) / dist4)
vinterp = vinterp / denom
END SUB

FUNCTION ray (a, b, c, x)
ray = a + b * x + c * x ^ 2
END FUNCTION
```